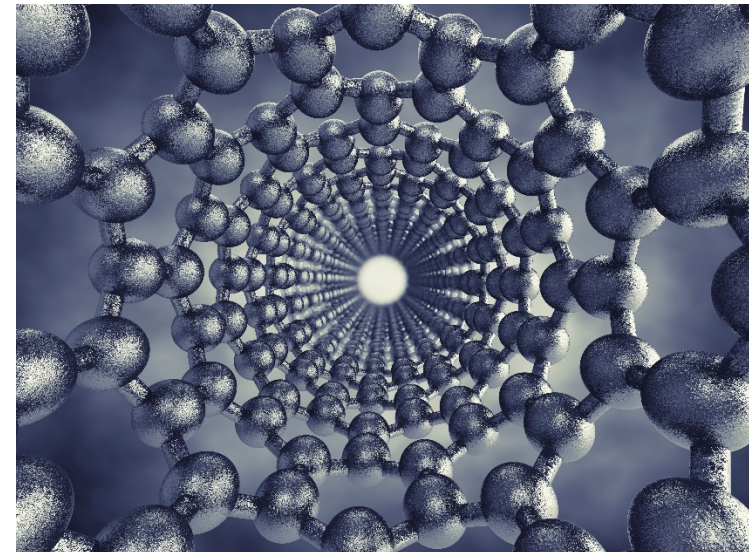


Simultaneous detection of multiple charged particles using a borosilicate nanopore-based sensor



Leyla Esfandiari, Ph.D.

Assistant professor of Electrical Engineering and Computing Systems

Assistant professor of Biomedical, Chemical & Environmental Engineering

Associate member of Cincinnati Cancer Center

College of Engineering and Applied Science

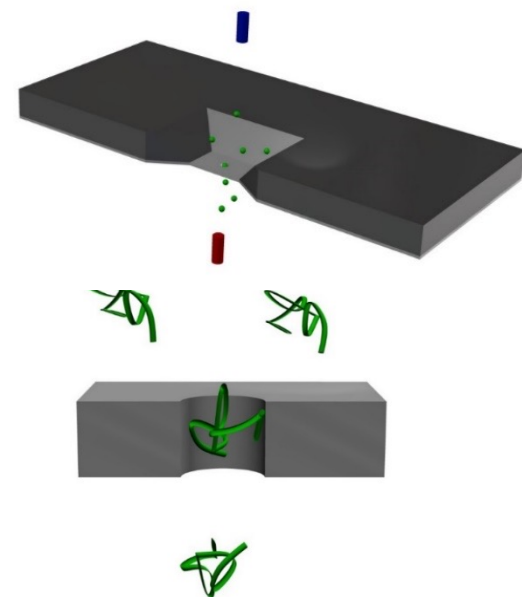
University of Cincinnati, USA

The need for point-of-care diagnostic

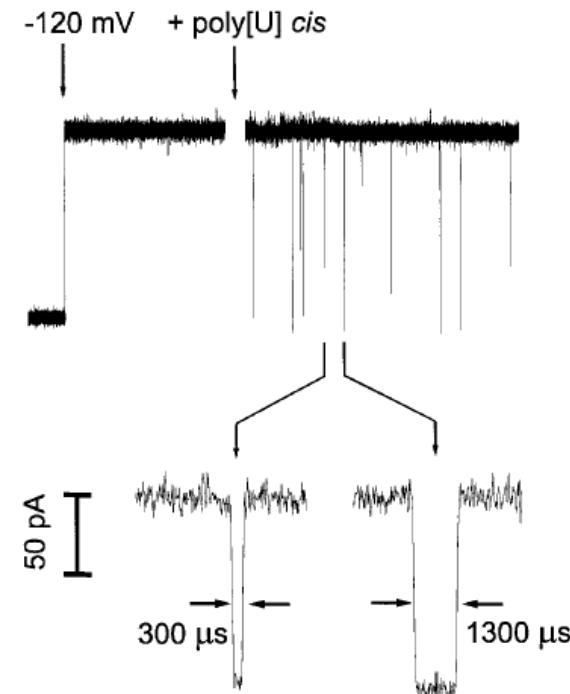


Nanopore sensor

Coulter Counter principle



Nanopore sequencing concept



Coulter Counter Operation

- ❖ Conductance changes as each particle goes through the pore
- ❖ The amplitude of the pulse is directly proportional to the volume of the particle
- ❖ Frequency of pulses is directly proportional to the concentration of the analytes

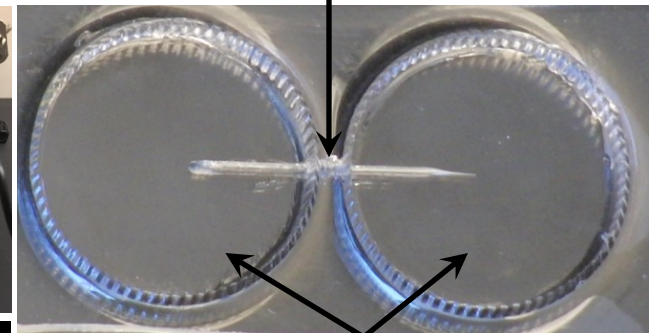
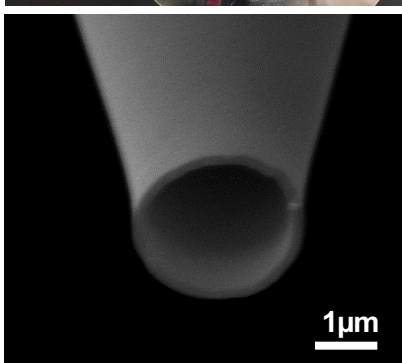
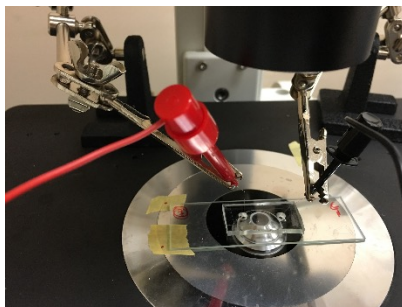
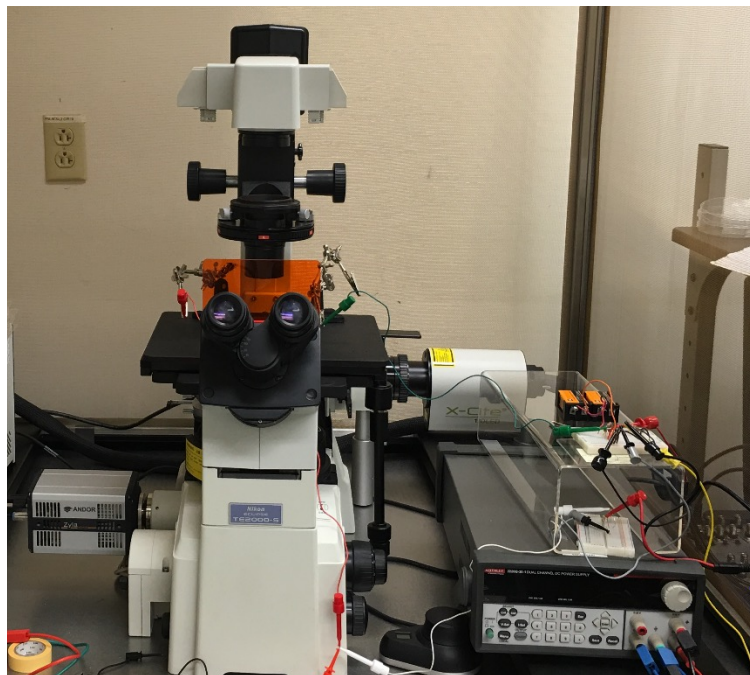
J.J. Kasianowicz, *PNAS*, vol. 93, pp. 13770-13773, 1996

Nanopore sequencing Challenges:

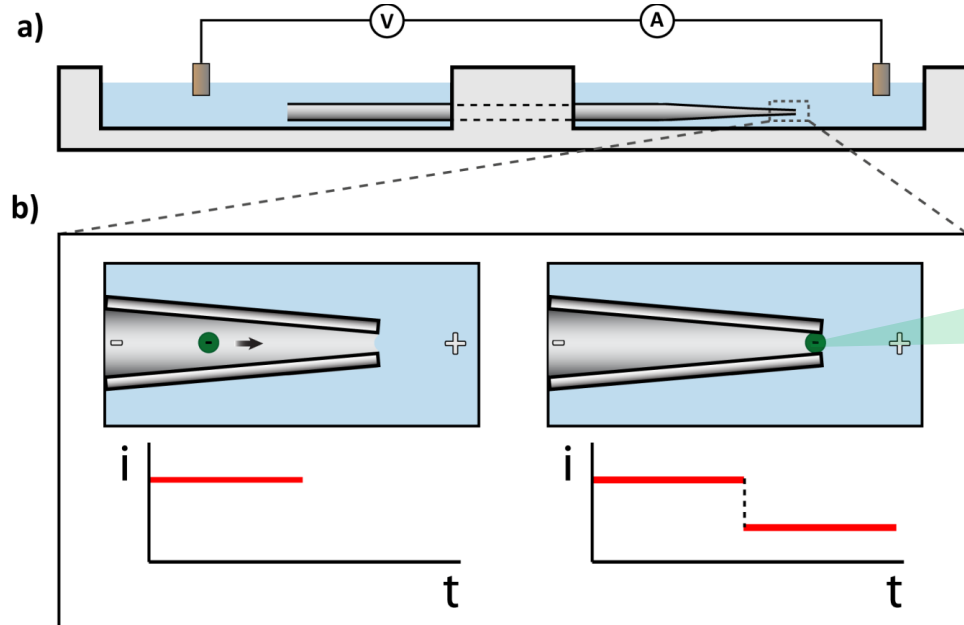
- ❖ Low temporal resolution
- ❖ Required sophisticated and expensive amplifier

Sensor Criteria

- i. Robust and inexpensive solid-state pore
- ii. Binary detection of target molecule
- iii. Easily detectable electrical signal with high signal to noise ratio
- iv. Intrinsic amplification of the signal



Sensor design



I. Solid-state pore (borosilicate glass)

II. Probe Substrate: Polystyrene spheres

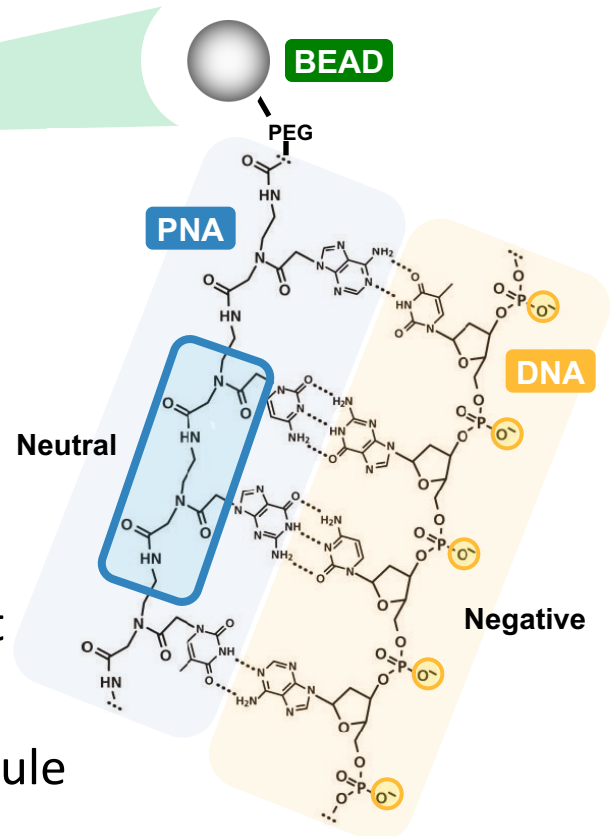
Electrophoretically **immobile** in the **absence** of target molecule

Electrophoretically **mobile** in **presence** of target molecule

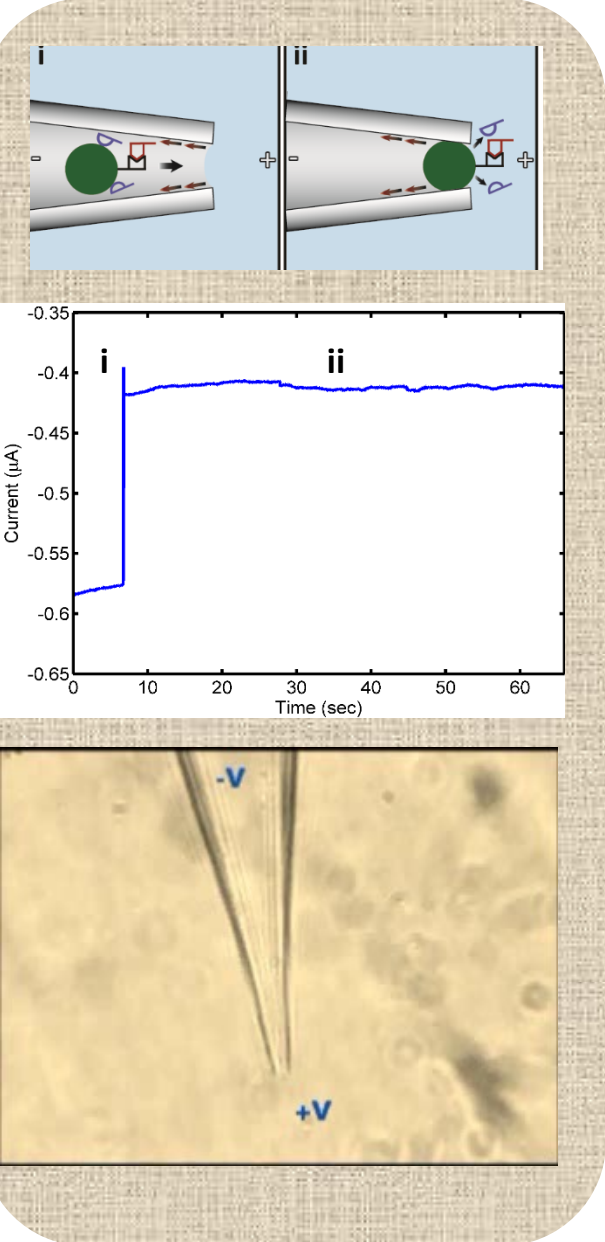
III. Probe molecule: **Peptide nucleic acids (PNAs)**

Electrically neutral

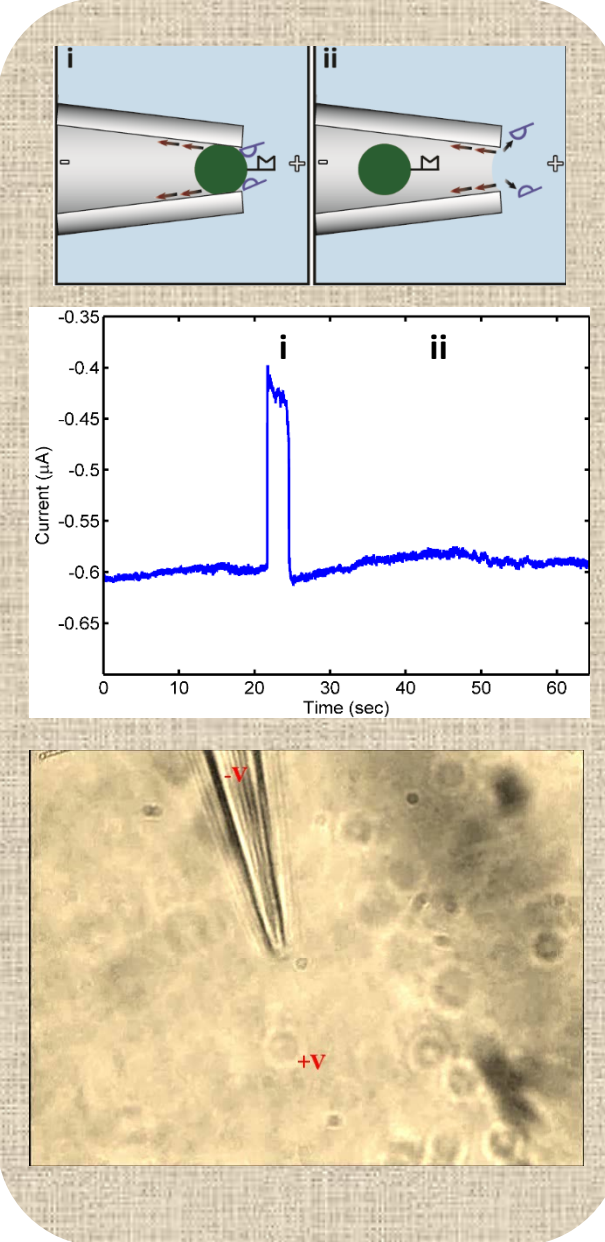
Complementary hybridization with DNA and RNA



Target



Control



Summary

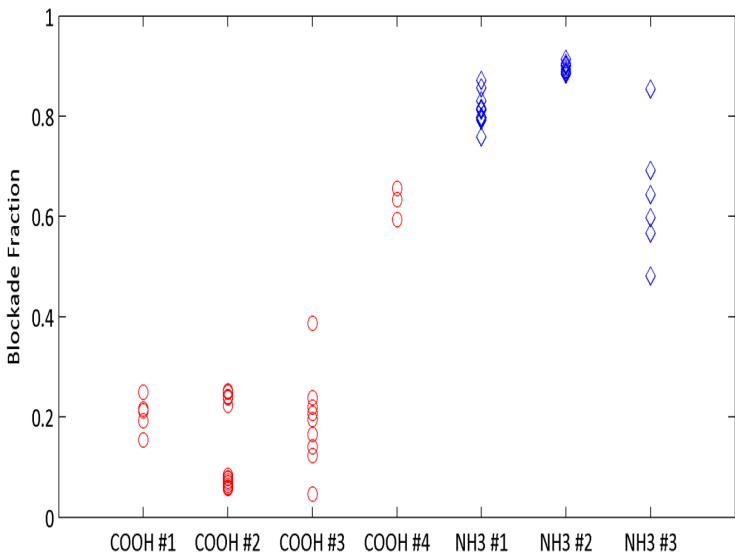
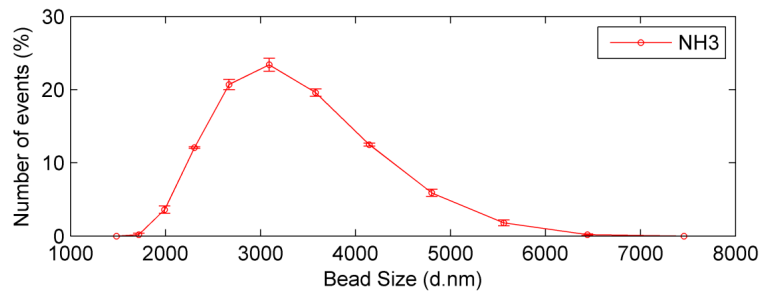
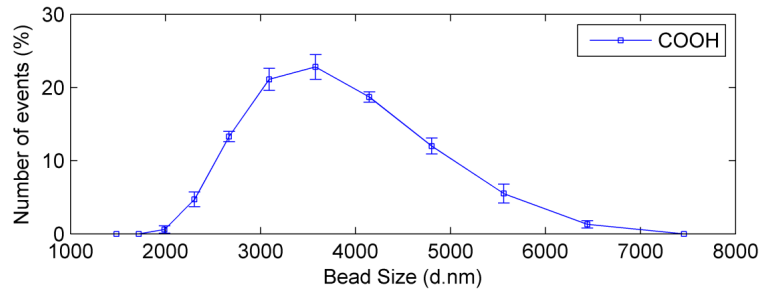
- ❖ Detection of Anthrax LF
- ❖ Single base mismatch specificity
- ❖ 10fM limit of detection
- ❖ PCR-independent
- ❖ Detection of bacterial species-specific 16S rRNA
- ❖ Only 3% false positive

L. Esfandiari et al., *J. Am. Chem. Soc.*, vol. 134, no. 38, pp. 15880–15886, 2012.

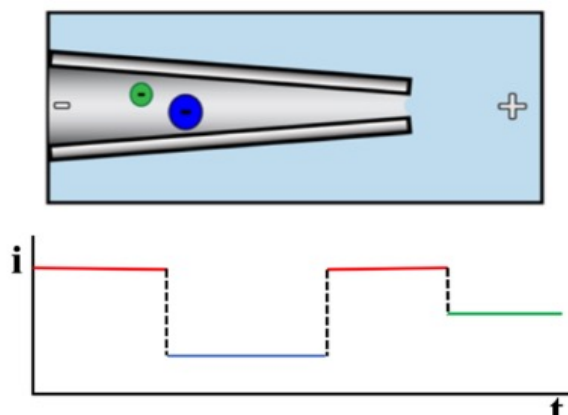
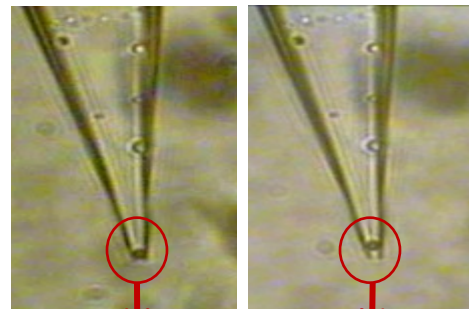
L. Esfandiari et al., *J. Anal. Chem.*, vol. 86, pp. 9638-9643, 2014

L. Esfandiari et al., *Biosensors.*, vol. 37, pp. 1-10, 2016

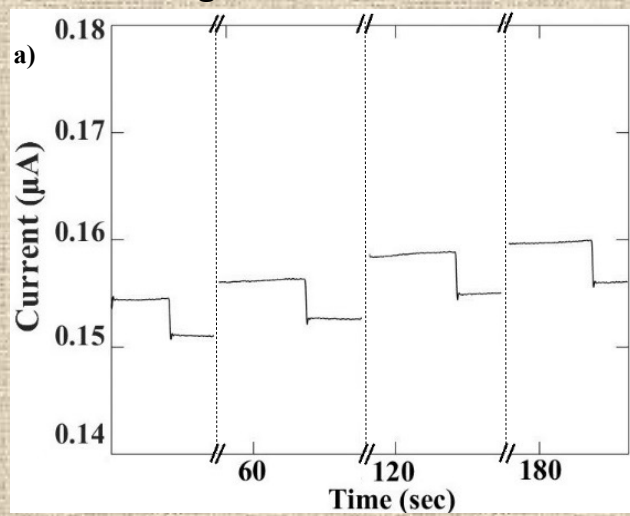
Multiplexing with one pore



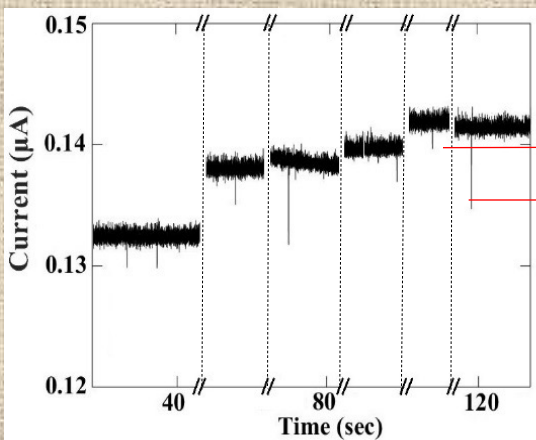
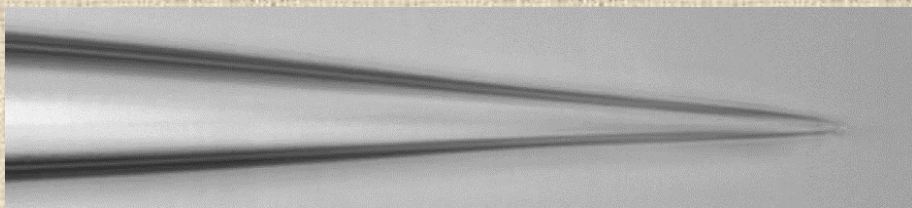
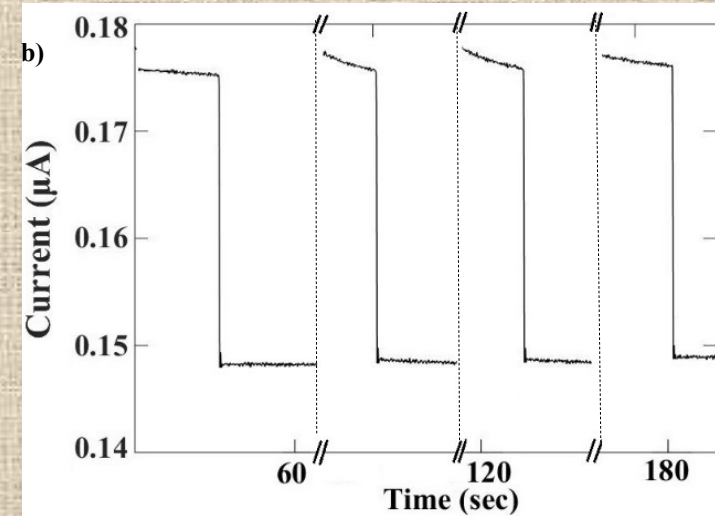
Two beads with different diameter



1 μ m COOH beads
Percentage of blockades 3.56%



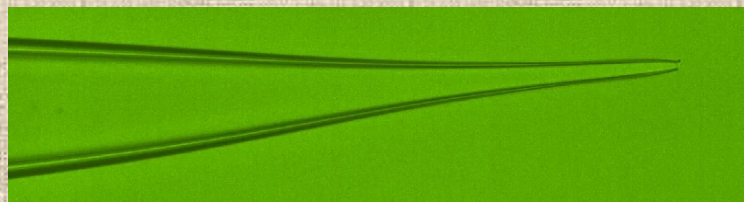
2.36 μ m COOH beads
Percentage of blockades 19.77%



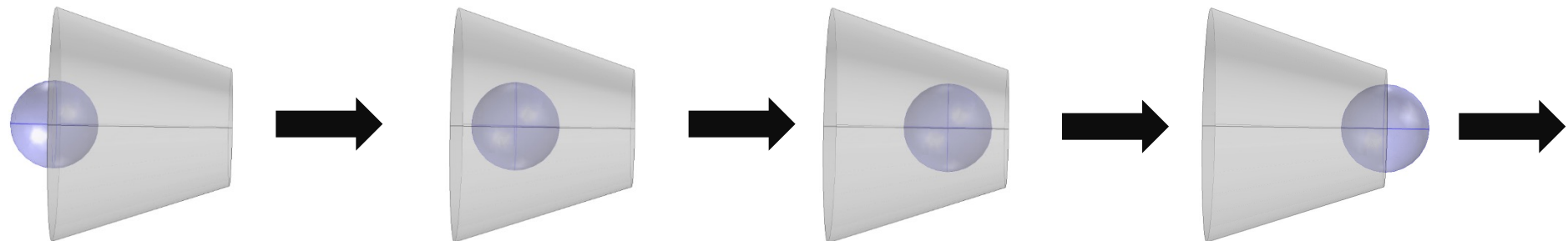
1.04 μ m beads
 $\Delta R: 5.2\%$

0.97 μ m beads
 $\Delta R: 2.2\%$

0.2 μ A
200ms



Theoretical modeling



Resistance Change Equation:

$$\Delta R = \frac{\rho}{\pi r_c \sqrt{1 - \sec^2 \alpha \left(\frac{r_p}{r_c}\right)^2}} \left[\tan^{-1} \frac{\tan \alpha + \sec^2 \alpha \frac{r_p}{r_c}}{\sqrt{1 - \sec^2 \alpha \left(\frac{r_p}{r_c}\right)^2}} - \tan^{-1} \frac{\tan \alpha - \sec^2 \alpha \frac{r_p}{r_c}}{\sqrt{1 - \sec^2 \alpha \left(\frac{r_p}{r_c}\right)^2}} \right] - \frac{2\rho \left(\frac{r_p}{r_c}\right)}{\pi r_c \sqrt{1 - \tan^2 \alpha \left(\frac{r_p}{r_c}\right)^2}}$$

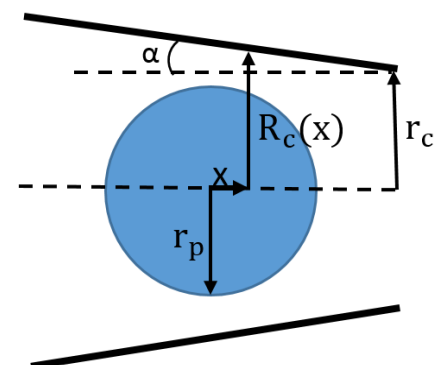
α , wall half angle

ρ , solution resistivity

r_c , radius of the capillary pore

r_p , radius of the particle

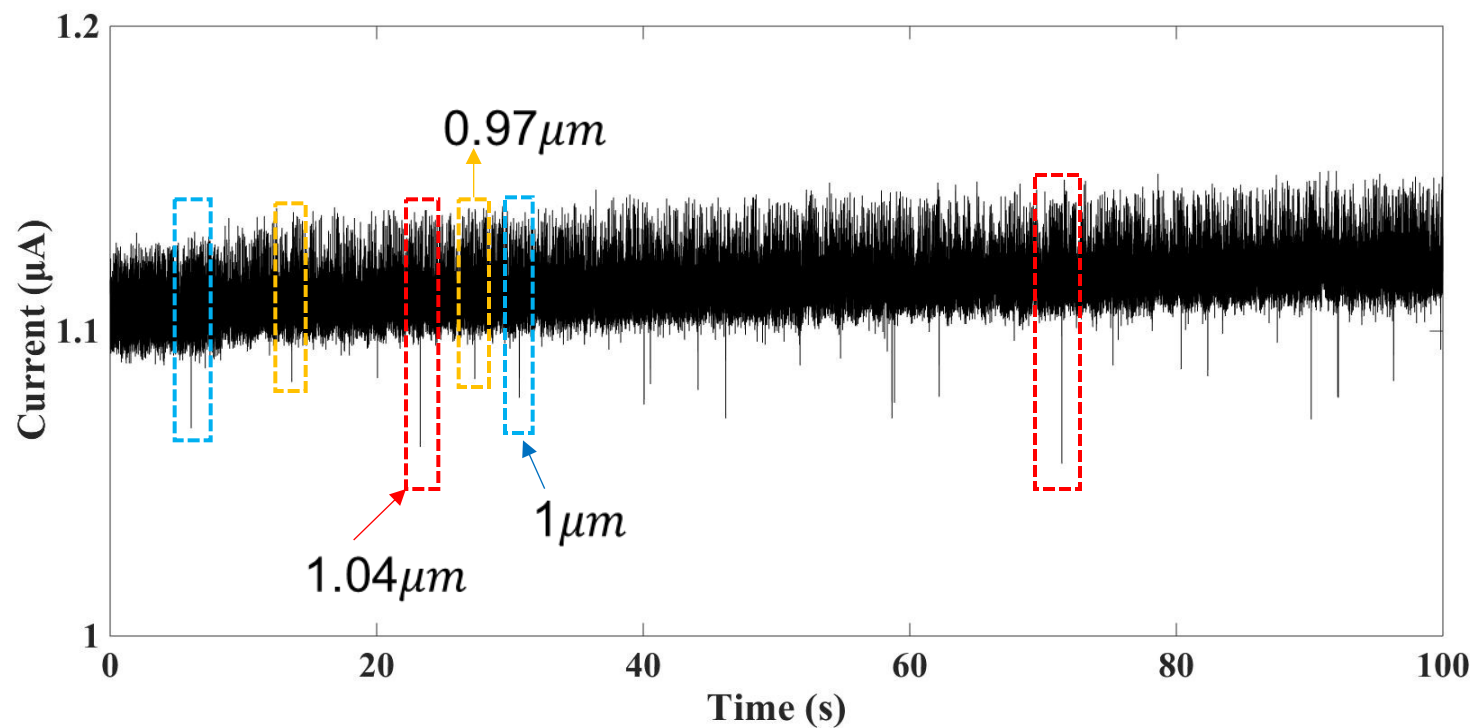
ΔR , change in resistance



Experimental	Theoretical
$\Delta R'_{1.04\mu m} = 8.6 M\Omega$	$\Delta R_{1.04\mu m} = 8.8 M\Omega$
$\Delta R'_{0.97\mu m} = 4.8 M\Omega$	$\Delta R_{0.97\mu m} = 5.2 M\Omega$

Gregg EC, Steidley KD. (1965). Electrical counting and sizing of mammalian cells in suspension. *Biophysical Journal*, 5, 393-405.

Multiplexing with three beads



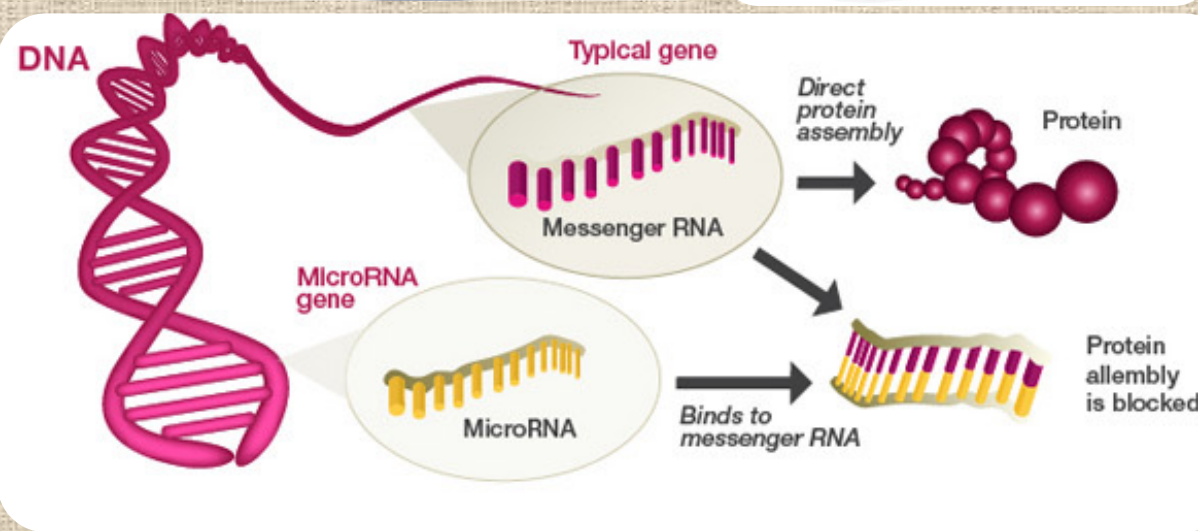
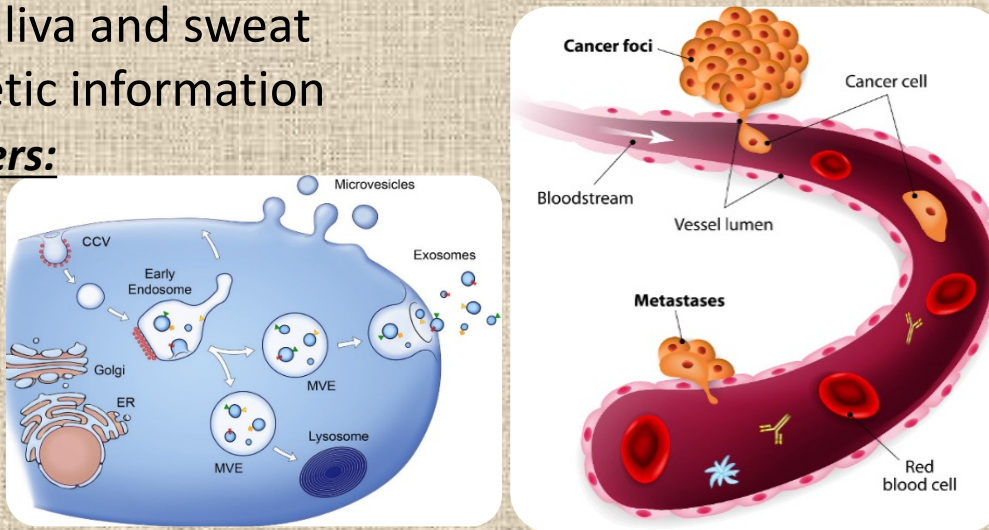
Bead diameter	ΔR
$1.04\mu\text{m}$	3.5%
$1\mu\text{m}$	2.2%
$0.97\mu\text{m}$	1.5%

Non-invasive, high-throughput point-of-care diagnostics

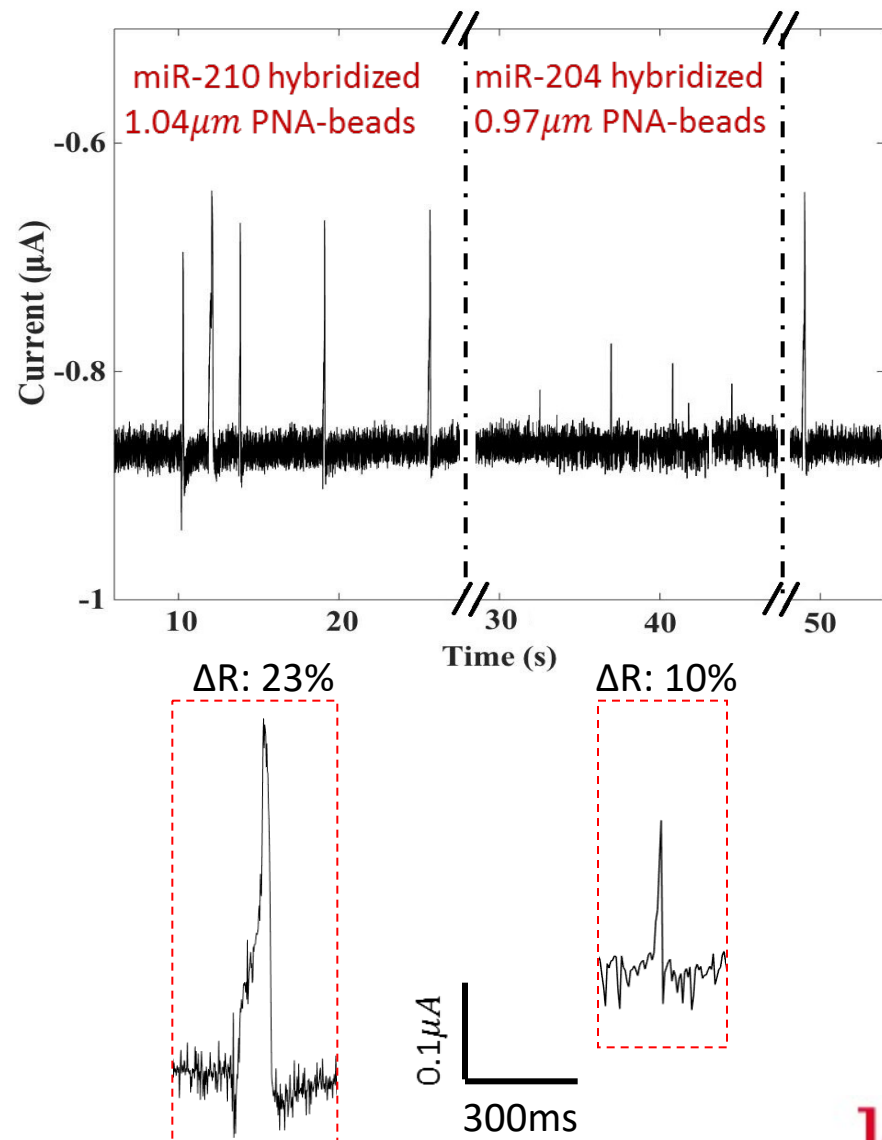
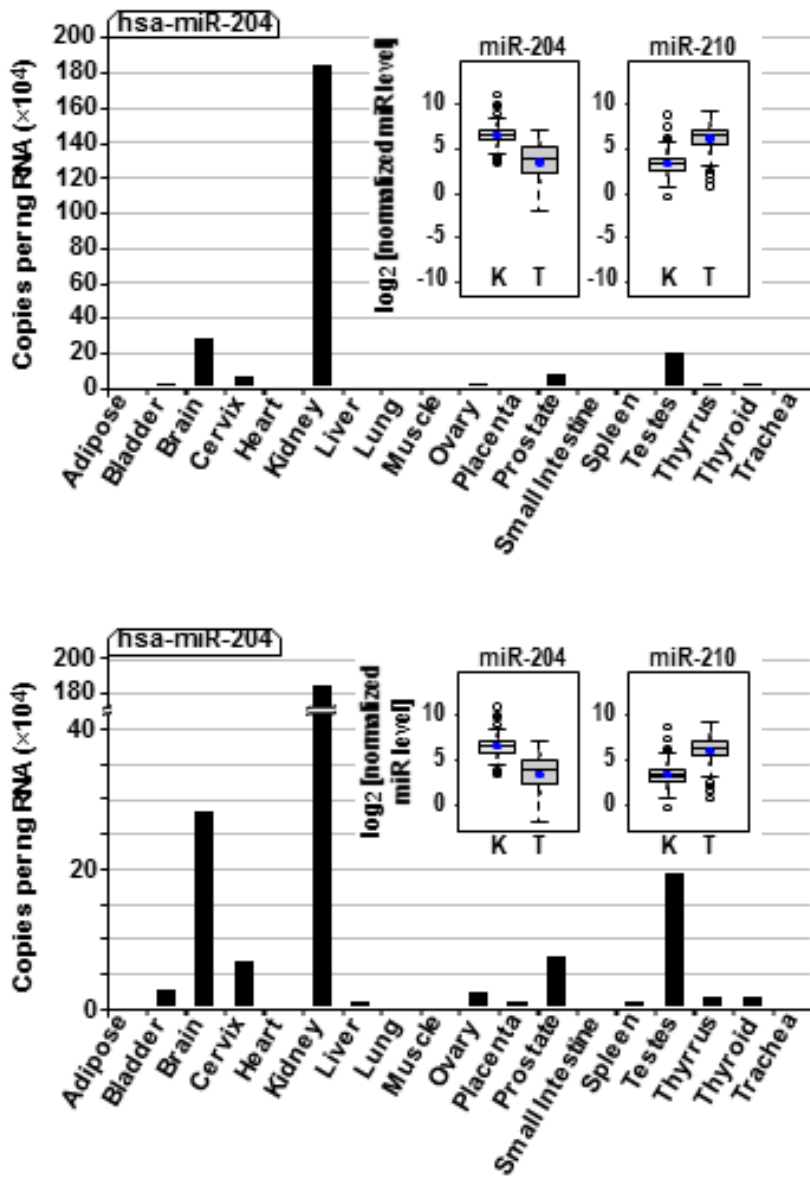
- ❖ Isolation of circulating micro-vesicles from body fluids such as serum, urine, saliva and sweat
- ❖ Analysis of genetic information

Circulating biomarkers:

Non-coding miRNAs



miR-210 & miR-204 Detection in cell renal cell carcinoma



Acknowledgement

Yuqian Zhang
EECE Ph.D. student

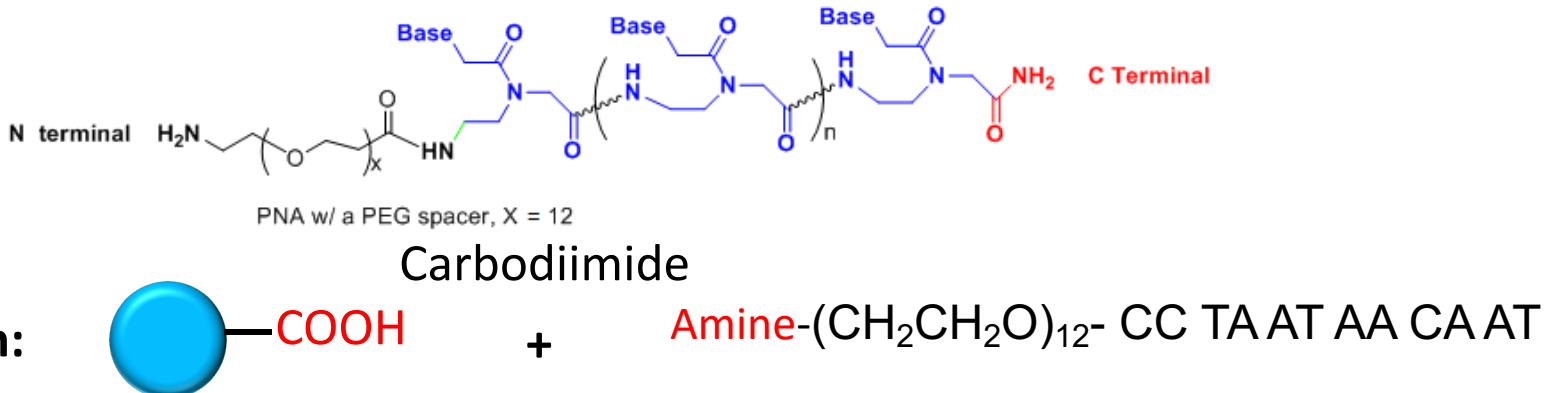


Maria F. Czyzyk-Krzeska, M.D., Ph.D.
Professor of Cancer biology



Assay development and characterization

(PNA)₁₂ complementary to **Anthrax lethal factor** sequence



COOH-beads Zeta potential : -102mV → PNA-beads Zeta potential: -7.39mV

Hybridization:

target: (ssDNA)₂₀ Anthrax LF + A₈

5'-GG AT TA TT GT TA AA AA AA AA-3'

PNA-beads ZP: -7.39mV → Target ssDNA-PNA-beads ZP : -51.1mV

Control: Anthrax LF + A₈ with single base mismatch

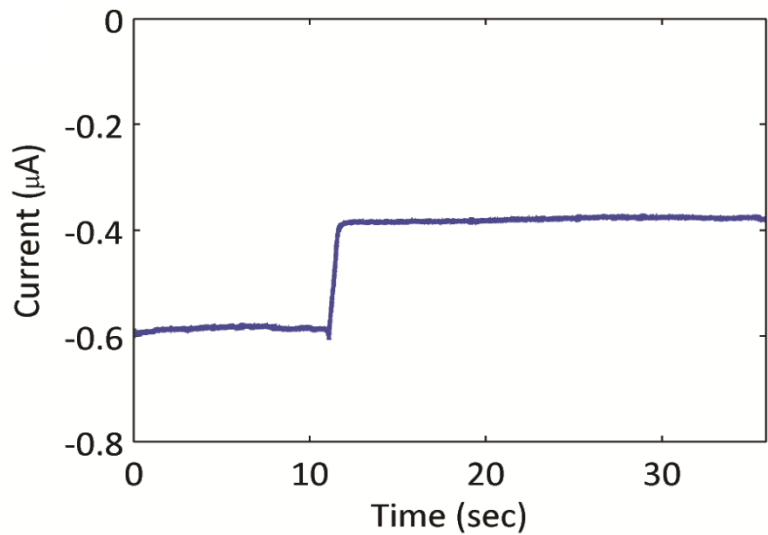
Hybridization:

5'-GG AT TC TT GT TA AA AA AA AA-3'

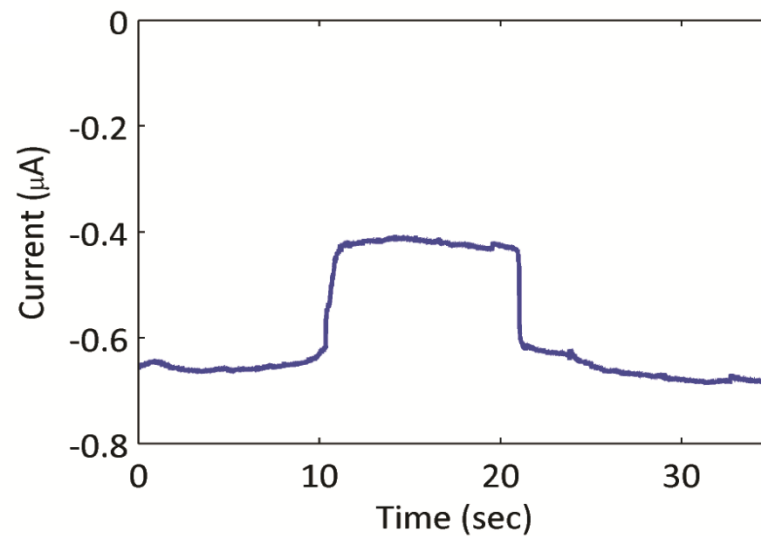
PNA-beads ZP: -7.39mV → Control ssDNA-PNA-beads ZP : -37.4mV

Sensor operation

Target

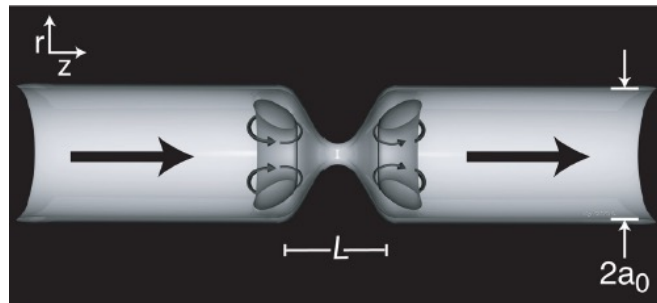
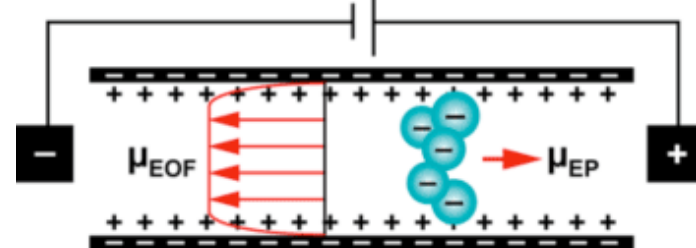


Control

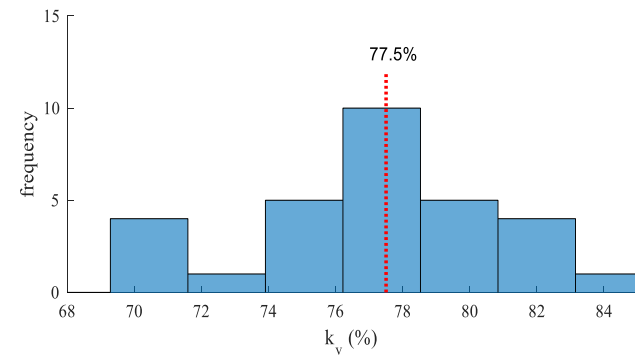
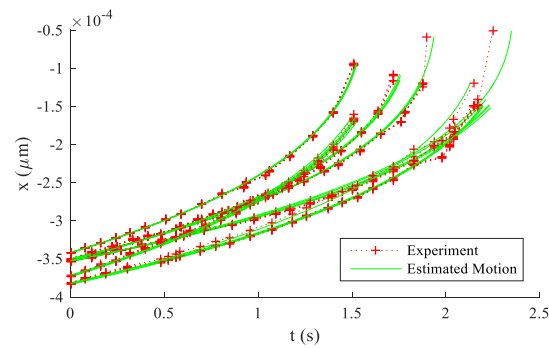
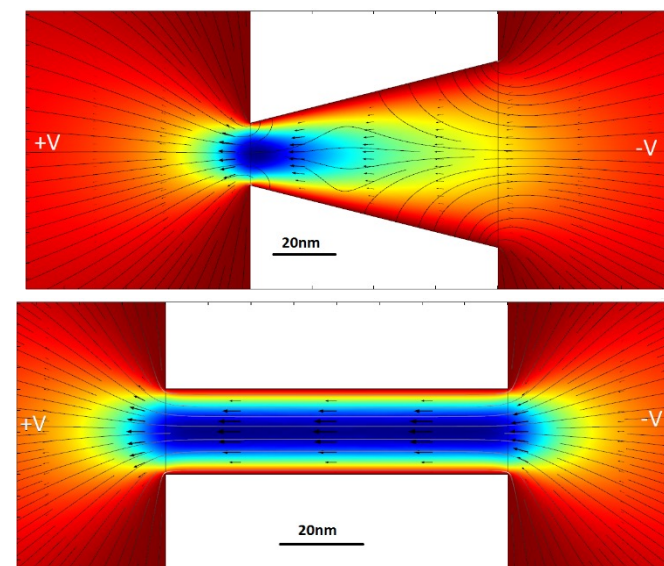


Fluid flow inside the pore

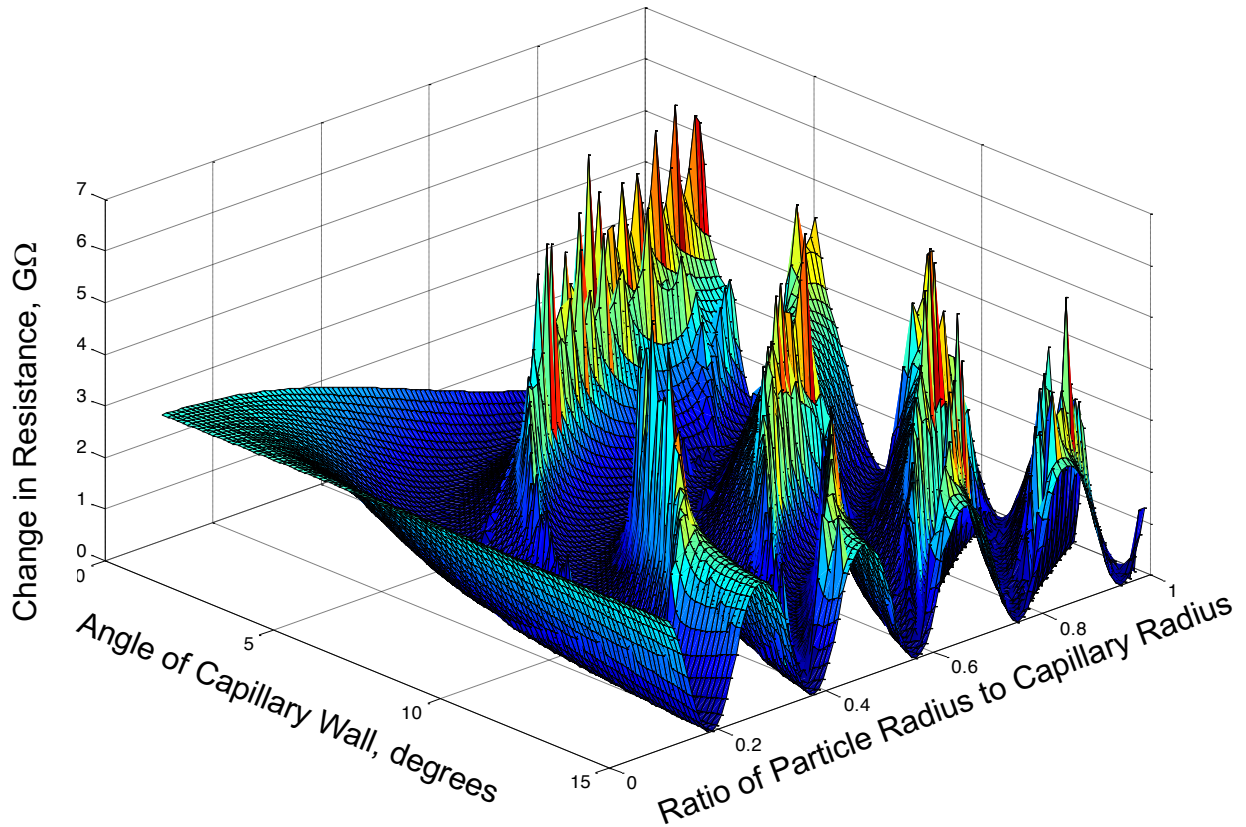
$$u_{EOF} = -\frac{\varepsilon \zeta E}{4\pi\mu} \quad u_{eo} = \frac{QE}{4\pi\mu r} \frac{\lambda_D}{r}$$



S.L.Park et al., *J. Colloid Interface Sci*, vol. 296, pp. 832–839, 2006.



Simulation



- Optimal Ratio: 0.3068
- Optimal Wall Angle: 11.84°
- Highest Resistance change: 6.132 $G\Omega$